

## Noise Induced State Transitions, Intermittency, and Universality in the Noisy Kuramoto-Sivashinsky Equation

M. Pradas,<sup>1</sup> D. Tseluiko,<sup>2</sup> S. Kalliadasis,<sup>1</sup> D. T. Papageorgiou,<sup>3</sup> and G. A. Pavliotis<sup>3</sup>

<sup>1</sup>*Department of Chemical Engineering, Imperial College London, London, SW7 2AZ, United Kingdom*

<sup>2</sup>*School of Mathematics, Loughborough University, Leicestershire, LE11 3TU, United Kingdom*

<sup>3</sup>*Department of Mathematics, Imperial College London, London, SW7 2AZ, United Kingdom*

(Received 5 November 2010; published 10 February 2011)

Consider the effect of pure additive noise on the long-time dynamics of the noisy Kuramoto-Sivashinsky (KS) equation close to the instability onset. When the noise acts only on the first stable mode (highly degenerate), the KS solution undergoes several state transitions, including critical on-off intermittency and stabilized states, as the noise strength increases. Similar results are obtained with the Burgers equation. Such noise-induced transitions are completely characterized through critical exponents, obtaining the same universality class for both equations, and rigorously explained using multiscale techniques.

DOI: 10.1103/PhysRevLett.106.060602

PACS numbers: 05.40.Ca, 02.50.-r, 05.45.-a, 47.54.-r

Most physical and technological settings are subject to random fluctuations, which are responsible for many intriguing and surprising phenomena [1]. These settings are often described by model spatially extended systems (SES), i.e., infinite-dimensional dynamical systems with space-time dependence and some stochastic forcing [2]. A widely studied example is the transition between different observed system *states* as the noise strength is increased beyond a critical value. For both pure temporal dynamical systems and fully nonlinear SES, it is well known that noise-induced transitions are due to multiplicative noise, i.e., noise whose amplitude depends on the fluctuating variable [1,3]. The presence of an additive noise, i.e., noise that does not depend on the state of the system, in addition to multiplicative one, has been shown to induce other phase transitions [4] while recently it has been shown that *pure additive noise*, i.e., thermal fluctuations, can stabilize linearly unstable solutions of SES [5,6]. However, a satisfactory and systematic description of the effects of thermal fluctuations on SES as well as a quantitative description of such effects in terms of critical-state transitions is still lacking.

In this Letter we report analytical and numerical evidence of pure additive noise-induced transitions in SES. As a main case study, we consider the noisy KS equation close to the primary bifurcation. We observe numerically a number of critical transitions by increasing the noise strength, including on-off intermittency, a crucial universal feature of many nonlinear systems close to criticality reflecting a transition from order or coherence to a disordered state (hence understanding the statistical properties of intermittency is crucial for the characterization of this transition). Our numerical observations can be fully explained in the context of a multiscale theory for SES.

*Noise in weakly nonlinear evolution equations.*—We consider the noisy KS equation

$$\partial_t u = -(\partial_x^2 + \nu \partial_x^4)u - u \partial_x u + \tilde{\sigma} \xi, \quad (1)$$

normalized to  $2\pi$  domains so that  $0 < \nu = (\pi/L)^2$ , where  $2L$  is the original length of the system, and with either homogeneous Dirichlet boundary conditions (DBC) or periodic boundary conditions (PBC). Equation (1), with and without the noise term, has attracted a lot of attention since it appears in a wide variety of physical phenomena and applications and it also serves as a canonical reference system of SES exhibiting spatiotemporal chaos or dissipative turbulence, e.g., reaction-diffusion systems and interfacial instabilities in fluid flows [7].

We shall assume throughout zero-mean solutions, and we study a randomly perturbed regime close to criticality by slightly increasing the domain size as  $L = \pi\sqrt{1 + \epsilon^2}$  so that we write  $\nu = 1 - \epsilon^2$  and  $\tilde{\sigma} = \epsilon\sigma$ , where  $\sigma$  represents the strength of the noise, with  $\epsilon$  being a bifurcation parameter; if  $\epsilon = 0$  all modes, except the neutral one, are stable with the system approaching its rest state as  $t \rightarrow \infty$ , and for  $0 < \epsilon < 1$ , a bifurcation occurs leading to a finite number of linearly unstable modes (in fact  $\lfloor 1/\sqrt{1 - \epsilon^2} \rfloor$  of them). The field  $u$  can then be projected onto the set of eigenfunctions  $\{e_k(x)\}$  for  $k = 1, 2, \dots$  of the linear operator  $\mathcal{L} = -\partial_x^2 - \partial_x^4$ , such that  $u(x, t) = \sum_k \hat{u}_k(t) e_k(x)$ , and in the limit  $\epsilon \rightarrow 0$ , only one single mode, namely  $\hat{u}_1(t)$ , will be unstable. We are interested in the dynamics of  $\hat{u}_1(t)$  when the stable modes,  $\hat{u}_k(t)$  for  $k \geq 2$ , are randomly forced, and, in particular, we focus on the case when only the first stable mode ( $\hat{u}_2$ ) is perturbed, so that the noise term in Eq. (1) is written as  $\xi(x, t) = \hat{\xi}_2(t) e_2(x)$ , where  $\hat{\xi}_2(t)$  is some uncorrelated Gaussian noise. This “highly degenerate noise” may give rise to a stabilization process of the unstable mode  $\hat{u}_1$  [5]. Typical snapshots of the spatiotemporal evolution of Eq. (1) subject to DBC with  $\sigma = 10$  and  $60$  are depicted in Fig. 1. The dynamic evolution of the first-mode amplitude,  $A(t) \equiv |\hat{u}_1(t)|$  is calculated for different noise strengths and boundary conditions.

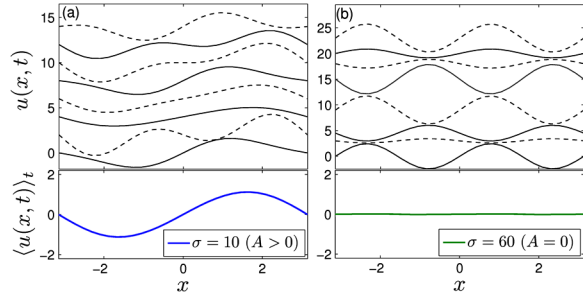


FIG. 1 (color online). Top panels show typical spatiotemporal evolution of the noisy KS equation solved with DBC for  $\epsilon = 0.1$  and  $\sigma = 10$  (a) and 60 (b) at time intervals  $\Delta t = 100$  depicted as solid-dashed lines. For clarity, the curves are arbitrarily shifted in the vertical direction. Bottom panels show the corresponding time average of  $u(x, t)$ .

In the case of DBC, the probability density function (PDF) of  $A(t)$  calculated for different values of  $\sigma$  is shown in Fig. 2(a). For  $\sigma = 15$  the amplitude is characterized by finite fluctuations that never reach zero [state I, top panel in the inset of Fig. 2(a)], and the PDF can be fitted to a function of the form  $P(A) = NA^{\alpha_1} \exp(-\delta A^2)$ . For  $\sigma = 35$ , the noise is strong enough to alter the behavior of the PDF, shifting its maximum position,  $A_{\max}$ , which can now reach zero (state II). We characterize this transition between I and II by computing  $A_{\max}$  for different  $\sigma$  [cf. Fig. 2(b)], obtaining  $A_{\max} \sim |\sigma^2 - 850|^{1/2}$  which gives a critical value of  $\sigma_1 \approx 29$ . Finally, as we increase  $\sigma$  up to the value  $\sigma = 51$  the first-mode is completely stabilized (state III), and the fluctuations eventually reach zero, defining a second critical transition at  $\sigma_{II} \approx 50$ . Such stabilization process can be clearly observed when the solution  $u(x, t)$  is averaged over time (cf. Fig. 1).

The middle panel in the inset of Fig. 2(a) demonstrates that state II is characterized by an *on-off intermittent* behavior of the amplitude fluctuations. Such intermittency can be characterized by studying the PDF of the waiting times  $T$  between two consecutive bursts, defined as large fluctuations above a given threshold, i.e.,  $A(t) > c_{th}$  [8]. Figure 3 shows the numerical results obtained by using two noise strengths. For  $\sigma = 50$ , close to the second critical point ( $\sigma_{II}$ ), the PDF of  $T$  is given by  $P(T) \sim T^{-\tau}$  with  $\tau = 3/2$ . Interestingly, this exponent has been ubiquitously found in many other physical systems that display avalanche or intermittent dynamics close to criticality, including neuronal activity in cortex, electroconvection of nematic liquid crystals or fluid flow in porous media [9]. For  $\sigma = 35$ , far from  $\sigma_{II}$ , the PDF is exponentially corrected. These results do not depend on the choice of the threshold value  $c_{th}$  (see inset of Fig. 3).

When the system is solved by imposing PBC, the first state transition occurs at  $\sigma \approx 36$  (cf. Fig. 4). Interestingly, as we increase the noise strength, the second critical transition is no longer observed, and the power-law regime of the amplitude PDF increases with an exponent that is asymptotically decreasing up to the value around  $-0.21$ .

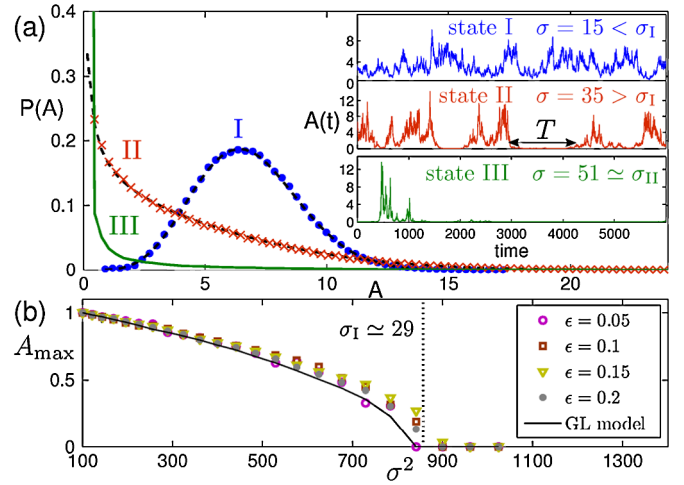


FIG. 2 (color online). Numerical results for Eq. (1) integrated on a  $[-\pi, \pi]$  domain with DBC. (a) PDF of the first-mode amplitude  $A(t) = |\hat{u}_1(t)|$  for  $\sigma = 15$  ( $\bullet$ ), 35 ( $\times$ ), and 51 (green solid line), with  $\epsilon = 0.1$ . Dashed lines correspond to a data fit using  $P(A) = NA^{\alpha_1} \exp(-\delta A^2)$ , where the fitted value  $\alpha_1$  is related to Eq. (5). The inset depicts typical fluctuations of the amplitude at each of the three states discussed in the text. (b) Maximum of the PDF as a function of  $\sigma^2$  for different values of  $\epsilon$ . The solid line corresponds to the theoretical solution obtained by solving numerically Eq. (3) with the coefficients of Eq. (4). All curves have been normalized to the corresponding minimum value at  $\sigma = 10$ .

Finally, the same analysis for both DBC and PBC has been performed for the noisy Burgers equation (used, for example, as a prototype for 1D turbulence, albeit without pressure gradient):  $\partial_t u = (\partial_x^2 + 1)u + \epsilon^2 u + u \partial_x u + \epsilon \sigma \xi$ . We obtain the values  $\sigma_1 \approx 6.4$  and  $\sigma_{II} \approx 9.5$  for the DBC case, including on-off intermittency with the same exponent for the waiting times' PDF (see Fig. 3). In the PBC case, we find  $\sigma_1 \approx 9.5$ , and as with the KS equation, the transition to state III is not observed either. This critical phenomenon occurring in both models reflects an underlying *universal* behavior. Our aim now is to explain all these numerical results using multiscale analysis (singular perturbation theory).

*Multiscale theory.*—We first analyze the noisy KS equation [10]. In the limit of  $\epsilon \ll 1$ , the system is close to the bifurcation point and Eq. (1) has two widely separated time scales, corresponding to the (stable) fast and (unstable) slow modes. Considering then the behavior of small solutions at time scales of  $O(\epsilon^{-2})$ , we define  $u(x, t) = \epsilon v(x, \epsilon^2 t)$  to transform Eq. (1) to

$$\partial_t v = -\epsilon^{-2}(\partial_x^2 + \partial_x^4)v + \partial_x^4 v - \epsilon^{-1}v \partial_x v + \epsilon^{-1}\sigma \epsilon_2 \hat{\xi}_2(t), \quad (2)$$

where we have assumed highly degenerate noise.

For DBC, the solution can be expanded in the basis  $\{e_k(x) = c_k \sin(kqx)\}$ , where  $q = \pi/L$ ,  $c_k$ 's are normalization constants, and the single dominant mode  $\hat{u}_1(t)$  is real and belongs to the null space of

$\mathcal{L} = -\partial_x^2 - \partial_x^4$ . Also, we stipulate that  $\xi(x, t) = \beta(t) \sin(2qx)$ , with  $\beta(t)$  being white noise,  $\langle \beta(t)\beta(t') \rangle = \delta(t-t')$ . To obtain the dominant mode amplitude equation we project the field  $v$  in Eq. (2) onto the null space of  $\mathcal{L}$  to get  $w_{\parallel} = \mathcal{P}_c v$ , where  $\mathcal{P}_c$  is the corresponding projector to the null space, and onto its orthogonal subspace (stable modes) to get  $w_{\perp} = (I - \mathcal{P}_c)u$ , where  $I$  is the identity operator. Equation (2), when written for the variables  $w_{\parallel}$  and  $w_{\perp}$  is of the form of a fast or slow system of stochastic differential equations (SDEs) for which homogenization theory applies [11]. By analyzing the corresponding Fokker-Planck equation using singular perturbation theory we obtain a closed equation for the distribution function of  $w_{\parallel}$  from which we can read off a one-dimensional stochastic differential equation that is valid in the limit  $\epsilon \rightarrow 0$ . The resulting equation for  $A(t) = |w_{\parallel}|$  is given by the GL equation with multiplicative Stratonovich noise:

$$\dot{A} = (1 + \gamma_1 \sigma^2)A - \gamma_2 A^3 + \gamma_3 \sigma A \beta(t), \quad (3)$$

where

$$\gamma_1 = -1/2688, \quad \gamma_2 = 1/48, \quad \gamma_3 = 1/24. \quad (4)$$

Equation (3) has been the subject of several studies (e.g. see Ref. [2] and references therein), and the corresponding stationary PDF for the random variable  $A$  is found to be [3]  $P(A) = NA^{\alpha_1} \exp(-\delta A^2)$ , with  $N$  a normalization constant, and

$$\begin{aligned} \alpha_1(\sigma) &= 2(1 + \gamma_1 \sigma^2)/(\gamma_3^2 \sigma^2) - 1, \\ \delta(\sigma) &= \gamma_2/(\gamma_3^2 \sigma^2). \end{aligned} \quad (5)$$

As noted in Ref. [1], depending on the location of the maxima of the above PDF, there may exist different states describing the amplitude  $A$ . The interesting point is that all the numerical states presented before can be achieved by

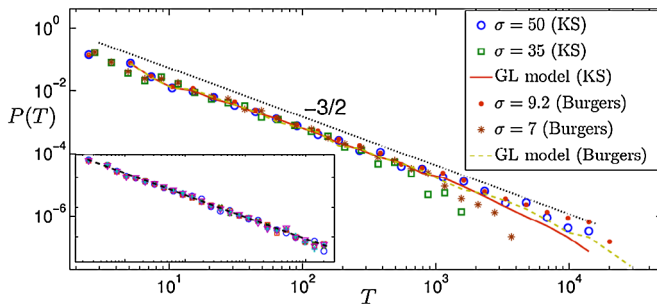


FIG. 3 (color online). PDF of the waiting times  $T$  between two consecutive bursts observed in the on-off intermittent state II corresponding to the DBC case. We solved both the KS equation, with  $\sigma = 35$  and  $50$ , and the Burgers equation, with  $\sigma = 9.2$  and  $\sigma = 7$ , by using  $\epsilon = 0.1$ . The solid and dashed lines correspond to the numerical solutions of the GL model, Eq. (3), by using the KS coefficients of Eq. (4) with  $\sigma = 50$ , and the corresponding Burgers coefficients with  $\sigma = 9$ , respectively. The dotted line is a data fit to  $P(T) \sim T^{-\tau}$  with  $\tau = 1.50 \pm 0.01$ . The inset shows the waiting times PDF in the KS equation with  $\sigma = 50$  and different values for the threshold, namely  $c_{\text{th}} = 0.05, 0.1, 0.2, 0.4,$  and  $0.8$ .

simply changing the value of  $\sigma$ . First, we observe that as long as  $\alpha_1 > 0$  the maximum of  $P(A)$  occurs at a finite value,  $A_{\text{max}} > 0$ , and then  $A$  is characterized by finite fluctuations around a mean value (state I). In contrast, for  $-1 < \alpha_1 \leq 0$ , the maximum is located at zero,  $A_{\text{max}} = 0$ , and the amplitude fluctuates intermittently between zero and a finite value (state II). These two states are separated by the critical value:

$$\sigma_{\text{I}} = (\gamma_3^2/2 - \gamma_1)^{-1/2}. \quad (6)$$

Note that for  $\gamma_1 > 0$ , this transition can only be observed as long as  $\gamma_3^2 > 2\gamma_1$ , while it is always observed for  $\gamma_1 < 0$ . By using the values of Eq. (4) we therefore obtain  $\sigma_{\text{I}} = 28.4$  in excellent agreement with the numerical observation shown at Fig. 2(b). In addition, the critical behavior can be characterized as  $A_{\text{max}} = |\sigma_{\text{I}}^2 - \sigma^2|^{1/2}/(\sigma_{\text{I}}\sqrt{\gamma_2})$  for  $\sigma \leq \sigma_{\text{I}}$ , and  $A_{\text{max}} = 0$  otherwise, so that  $A_{\text{max}}$  and  $\sigma^2$  are the order and control parameter, respectively, describing the critical transition. By solving numerically Eq. (3) with the coefficients of Eq. (4) for different  $\sigma$ , we find very good agreement between analytical and numerical results [cf. Fig. 2(b)]. If  $\gamma_1 < 0$ , a second transition occurs when  $\alpha_1 \leq -1$ . The PDF cannot be normalized and it is given by a Dirac delta function,  $P(A) = \delta(A)$ , describing a completely stabilized state with  $A = 0$  (state III). The critical value  $\sigma_{\text{II}}$  for this second transition is:

$$\sigma_{\text{II}} = \sqrt{1/|\gamma_1|}, \quad (7)$$

yielding  $\sigma_{\text{II}} = 51.8$ , in excellent agreement with the numerical results [cf. Fig. 2(a)]. To obtain analytically the statistical properties of the waiting times  $T$ , we assume that in a regime close to the critical point ( $\sigma \lesssim \sigma_{\text{II}}$ ) the initial

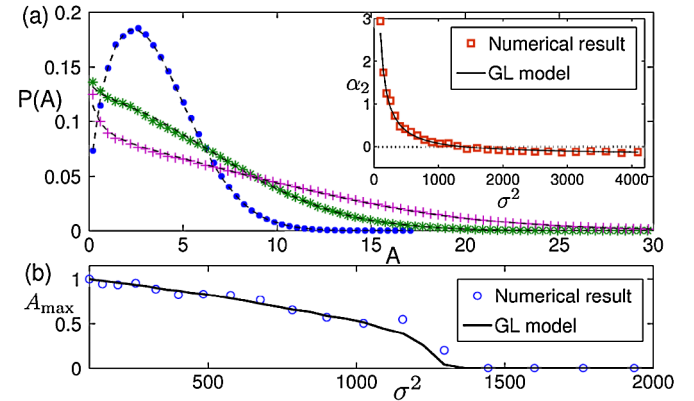


FIG. 4 (color online). Numerical results for the stochastic KS equation (1) integrated on a  $[-\pi, \pi]$  domain with PBC. (a) PDF of the first-mode amplitude for  $\sigma = 25$  ( $\bullet$ ),  $45$  ( $*$ ), and  $65$  ( $+$ ), with  $\epsilon = 0.025$ . Dashed lines correspond to a data fit using  $P(A) = NA^{\alpha_2} \exp(-\delta'A^2)$ . The inset shows the value of the fitted exponent  $\alpha_2$  as a function of  $\sigma^2$  compared to the analytical solution (solid line) given by Eq. (10). (b) Maximum of the PDF as a function of  $\sigma^2$  normalized with the value corresponding at  $\sigma = 10$ . The solid line corresponds to the numerical solution of Eqs. (8) and (9), by using Eq. (4).

value of  $A$  is below a small given threshold  $c_{\text{th}}$ , and we ask for the probability  $P(T)$  that at time  $T$  the amplitude reaches the threshold for the first time. In this close-to-zero state we can neglect the nonlinear term in Eq. (3), and we introduce the transformation  $y = \log A$  obtaining  $\dot{y} = 1 + \gamma_1 \sigma^2 + \gamma_3 \sigma \beta(t)$  with  $y \in (-\infty, \log c_{\text{th}}]$ . We thus recognise an underlying dynamics described by the well-known first-passage properties of the random walk [12], giving rise in our case to the long-time behavior  $P(T) \sim T^{-3/2} \exp(-T/T_0)$  with  $T_0 = [2\gamma_3 \sigma / (1 + \gamma_1 \sigma^2)]^2$ , from which in the critical point  $\sigma = \sigma_{\text{II}}$  we recover the numerically observed pure power-law (cf. Fig. 3). Clearly, the exponent  $-3/2$  will be universally observed in any SES whose dominant mode is described by Eq. (3).

Consider now the case with PBC. The solution is then expanded in the exponential Fourier basis  $\{e_k(x) = c_k \exp(ikqx)\}$ , for  $k = 0, \pm 1, \pm 2, \dots$ , and the single dominant mode has two components:  $\hat{u}_1(t)e_1(x) = y_1 \sin(qx) + z_1 \cos(qx)$ . The noise is now given as  $\xi(x, t) = \beta_1(t) \sin(2qx) + \beta_2(t) \cos(2qx)$ , where  $\beta_1(t)$  and  $\beta_2(t)$  are uncorrelated white random variables. By applying our multiscale methodology we obtain

$$\dot{y}_1 = (1 + 2\gamma_1 \sigma^2)y_1 - \gamma_2 y_1 A^2 + 2\gamma_3 \sigma A \beta_1, \quad (8)$$

$$\dot{z}_1 = (1 + 2\gamma_1 \sigma^2)z_1 - \gamma_2 z_1 A^2 + 2\gamma_3 \sigma A \beta_2, \quad (9)$$

where  $A(t) = \sqrt{y_1^2 + z_1^2}$ , and  $\gamma_1$ ,  $\gamma_2$ , and  $\gamma_3$  are given by Eq. (4). The stationary joint PDF for the two variables,  $G(y_1, z_1)$ , is obtained by computing the corresponding stationary two-dimensional Fokker-Planck equation, yielding  $G(y_1, z_1) \propto (y_1^2 + z_1^2)^{\alpha'_1/2} \exp[-\delta'(y_1^2 + z_1^2)]$ , where  $\alpha'_1$  and  $\delta'$  are obtained from the expressions in Eq. (5) by replacing  $\gamma_1$  and  $\gamma_3$  with  $2\gamma_1$  and  $2\gamma_3$ , respectively. To study the behavior of  $P(A)$ , we move to a polar coordinate system  $(A, \theta)$  and impose the condition  $G(y_1, z_1) dy_1 dz_1 = P(A, \theta) dA d\theta$ , getting  $P(A) \propto A^{\alpha_2} \exp(-\delta' A^2)$ , with

$$\alpha_2(\sigma) = \alpha'_1 + 1 = (1 + 2\gamma_1 \sigma^2) / (2\gamma_3^2 \sigma^2). \quad (10)$$

We first note that state transitions can only occur iff  $\gamma_1 < 0$ , with the critical values:  $\sigma_{\text{I}} = \sqrt{1/2|\gamma_1|}$ , and  $\sigma_{\text{II}} = [2(|\gamma_1| - \gamma_3^2)]^{-1/2}$ . Interestingly, the second transition can only occur as long as  $\gamma_3^2 < |\gamma_1|$ . Otherwise, state III is never observed, and the distribution tends to  $P(A) \sim A^{\alpha_\infty}$  as  $\sigma \rightarrow \infty$ , with  $\alpha_\infty = -|\gamma_1|/\gamma_3^2$ . By using Eq. (4), the first transition occurs at  $\sigma_{\text{I}} = 36.3$ , while the second transition cannot be observed with  $\alpha_\infty = -0.21$ , in excellent agreement with the numerical results (cf. Fig. 4). Finally, when this formalism is applied to the Burgers equation, we obtain the coefficients  $\gamma_1 = -1/88$ ,  $\gamma_2 = 1/12$ , and  $\gamma_3 = 1/6$ , giving rise to  $\sigma_{\text{I}} = 6.3$  and  $\sigma_{\text{II}} = 9.4$  for DBC, and  $\sigma_{\text{I}} = 9.4$  for PBC, in excellent agreement with the numerical results. As with the KS equation, we have  $\gamma_3^2 > |\gamma_1|$ , and the second transition is not observed for PBC either.

To conclude, we have presented clear evidence of critical transitions in SES induced by pure additive noise.

We have focused on the KS equation and by adding a stochastic forcing acting on the first stable mode, we have provided a detailed and systematic investigation of the transitions between different states. In particular, by using multiscale analysis for SDEs, we have analytically described the different critical-state transitions that are undergone by the amplitude of the unstable mode, including on-off intermittency and stabilized states, that we have also observed numerically in both the KS and Burgers equations. Moreover, the critical exponents for both SES are the same, and hence they belong to the same universality class. This is in accordance with Yakhot's conjecture [13]. We believe that our results will motivate further analytical and numerical studies on the effect of additive noise in general SES.

We thank Christian Ruyer-Quil for useful discussions. We acknowledge financial support from EU-FP7 ITN Multiflow. D.T.P. was partly supported by NSF Grant DMS-0707339.

- 
- [1] W. Horsthemke and R. Lefever, *Noise-Induced Transitions* (Springer, Berlin, 1984).
  - [2] F. Sagués, J. M. Sancho, and J. García-Ojalvo, *Rev. Mod. Phys.* **79**, 829 (2007).
  - [3] M. C. Mackey, A. Longtin, and A. Lasota, *J. Stat. Phys.* **60**, 735 (1990).
  - [4] A. A. Zaikin, J. García-Ojalvo, and L. Schimansky-Geier, *Phys. Rev. E* **60**, R6275 (1999).
  - [5] D. Blömker, M. Hairer, and G. A. Pavliotis, *Nonlinearity* **20**, 1721 (2007).
  - [6] A. Hutt, A. Longtin, and L. Schimansky-Geier, *Phys. Rev. Lett.* **98**, 230601 (2007); A. Hutt, *Europhys. Lett.* **84**, 34003 (2008); D. Obeid, J. M. Kosterlitz, and B. Sandstede, *Phys. Rev. E* **81**, 066205 (2010).
  - [7] Y. Kuramoto and T. Tsuzuki, *Prog. Theor. Phys.* **55**, 356 (1976); D. T. Papageorgiou, C. Maldarelli, and D. S. Rumschitzki, *Phys. Fluids A* **2**, 340 (1990); C. Duprat *et al.*, *Phys. Rev. Lett.* **103**, 234501 (2009); D. Tseluiko *et al.*, *Physica (Amsterdam)* **239D**, 2000 (2010); Y.-S. Smyrlis and D. T. Papageorgiou, *Proc. Natl. Acad. Sci. U.S.A.* **88**, 11 129 (1991).
  - [8] J. F. Heagy, N. Platt, and S. M. Hammel, *Phys. Rev. E* **49**, 1140 (1994).
  - [9] P. Bak, *How Nature Works: The Science of Self-Organized Criticality* (Copernicus, New York, 1996); J. M. López, M. Pradas, and A. Hernández-Machado, *Phys. Rev. E* **82**, 031127 (2010).
  - [10] The formalism is of much wider applicability and could be easily extended to other prototypes.
  - [11] G. A. Pavliotis and A. M. Stuart, *Multiscale Methods: Averaging and Homogenization* (Springer, New York, 2008).
  - [12] S. Redner, *A Guide to First-Passage Processes* (Cambridge University Press, Cambridge, England, 2001).
  - [13] V. Yakhot, *Phys. Rev. A* **24**, 642 (1981); K. Ueno, H. Sakaguchi, and M. Okamura, *Phys. Rev. E* **71**, 046138 (2005).